



Microarticle

Germanium antimony quantum dots morphology and Raman spectroscopy fabricated by inert gas condensation

Ishaq Musa^{a,*}, Naser Qamhieh^b, Khadija Said^b^a Department of Physics, Palestine Technical University-Kadoorie, Tulkarm, P.O. Box 7, Palestine^b Department of Physics, UAE University, Al-Ain, P.O. Box 15551, United Arab Emirates

ARTICLE INFO

Keywords:

Ge-Sb quantum dots
Atomic force microscopy
Magnetron sputtering
Raman spectroscopy

ABSTRACT

Phase change materials (PCM) based on nanostructure are attractive interest for non-volatile memory due to their high data-storage density and low power consumption. Germanium antimony (Ge-Sb) quantum dots (QDs) with tunable size and density have been fabricated on mica, silicon, and quartz glass substrates by magnetron sputtering with inert gas condensation. The deposition time rate plays an important role in the formation of the monodisperse or aggregate quantum dots. The dots' morphology, in terms of size and density as observed by atomic force microscopy (AFM) strongly depends on the deposition time rate. The size of QDs was observed by (AFM) images topography between 1.6 and 3.2 nm. Raman spectroscopy measurements reveal that Ge-Sb phonon at 250 cm^{-1} (Lo mode) and 220 cm^{-1} (To mode). Also, strong Sb-Sb crystallized peaks positioned at about 145 cm^{-1} and 110 cm^{-1} is observed.

Introduction

Phase change flash memory is a potential technology that used phase change materials [1]. Intensive research in the last few decades in chalcogenide materials such as, GeSbTe [2], GeTe, GeSbS [3], and GeSb [4] has attracted the researchers interest; because of the desirable physical properties that utilizes the switching between amorphous and crystalline phases. This properties makes the chalcogenide materials important for various technological applications such as, optical storage discs [5] and non-volatile random access memory (NVRAM) [6]. In addition, phase change materials can store and retrieve data 100 times faster than traditional flash memory [7]. The operation of NVRAM utilizes the properties of nanostructures such as nanoparticles and nanowires. These types of

NVRAM are suitable for next generation memories due to their unique size-dependent properties. Nanomaterials engineering can provide smaller devices than those currently available in bulk materials. Recently, one dimension (1-D) and zero dimension (0-D) nanostructures has become core of research in nanotechnology due to their interesting properties. These properties are essentially linked with low dimensionality and small diameters, which may lead to unique applications in different nano-scale devices such as high data storage [8], high write and read speeds, and low power consumption [9]. In the last decade, many different techniques were employed to produce chalcogenide thin films and nanostructures with different sizes and shapes.

These techniques include: sputtering [10], thermal evaporation [11], sol-gel [12], pulse laser [13], chemical vapor deposition (CVD) [14], and magnetron sputtering with inert gas condensation (IGC) [15]. Among of these methods, the magnetron sputtering with (IGC) is very attractive due to the tunable selected size of nanoparticles and density. In addition, Magnetron sputtering with (IGC) method has advantage compared to other techniques, because the elements with different vapor pressures can be synthesized with good compositional homogeneity. Also, the conventional sputtering of thin films is done at very low pressures ($\cong 10^{-3}$ mbar), while the synthesize nanoparticles with (IGC) are working at pressures of ($\cong 10^{-1}$ mbar). Moreover, when changing the gas pressure, the particle size can be changed which cannot be achieved in thermal evaporation method [16].

In this paper, we present Raman scattering spectroscopy results for $\text{Ge}_{15}\text{Sb}_{85}$ quantum dots that were deposited by magnetron sputtering with inert gas condensation method. We could also provide information regarding optimal deposition conditions for size and density of quantum dots.

Experimental methods

The GeSb quantum dots (QDs) with different sizes were produced by magnetron sputtering with inert gas condensation (Mantis Deposition Ltd.). The depositions of QDs carry out on mica and Si substrates with different time deposition (2 and 10 mints). In briefly, $\text{Ge}_{15}\text{Sb}_{85}$

* Corresponding author.

E-mail address: i.musa@ptuk.edu.ps (I. Musa).<https://doi.org/10.1016/j.rinp.2019.102311>

Received 5 April 2019; Received in revised form 23 April 2019; Accepted 23 April 2019

Available online 24 April 2019

2211-3797/© 2019 Published by Elsevier B.V. This is an open access article under the CC BY-NC-ND license

<http://creativecommons.org/licenses/by-nc-nd/4.0/>.

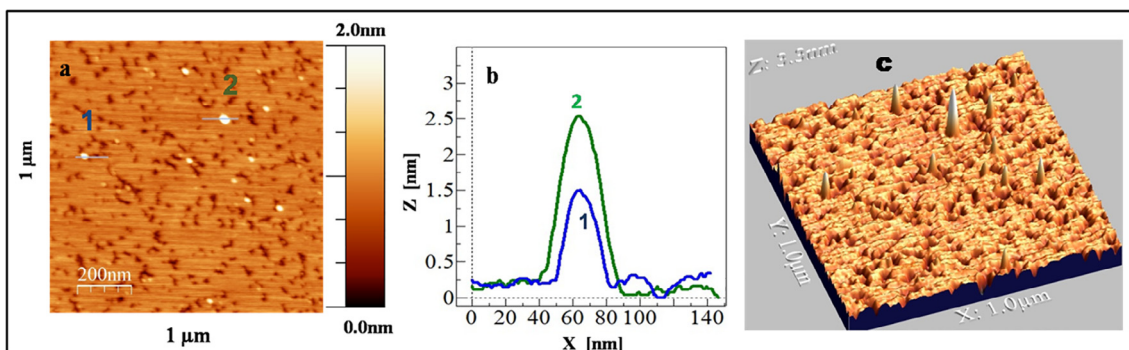


Fig. 1. $1 \mu\text{m} \times 1 \mu\text{m}$ AFM topographic image of $\text{Ge}_{15}\text{Sb}_{85}$ quantum dots on mica for short time(2 min) deposition and low densities (a) and line profiles for the 2 separate quantum dots identified in the image at image a, (b). Three-dimensional projection of QDs (c).

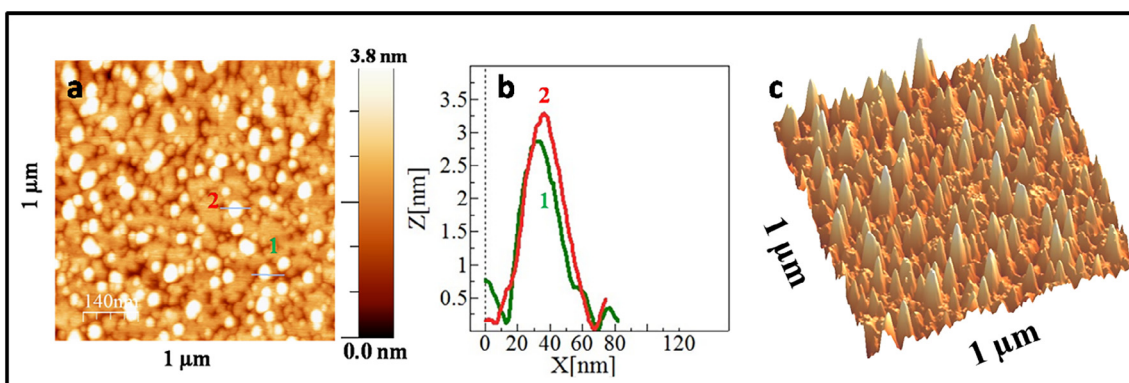


Fig. 2. $1 \mu\text{m} \times 1 \mu\text{m}$ AFM topographic image of $\text{Ge}_{15}\text{Sb}_{85}$ quantum dots on mica for long time (6 min) deposition and high densities (a) and line profiles for the 2 separate quantum dots identified in the image at a, (b). Three-dimensional projection of QDs (c).

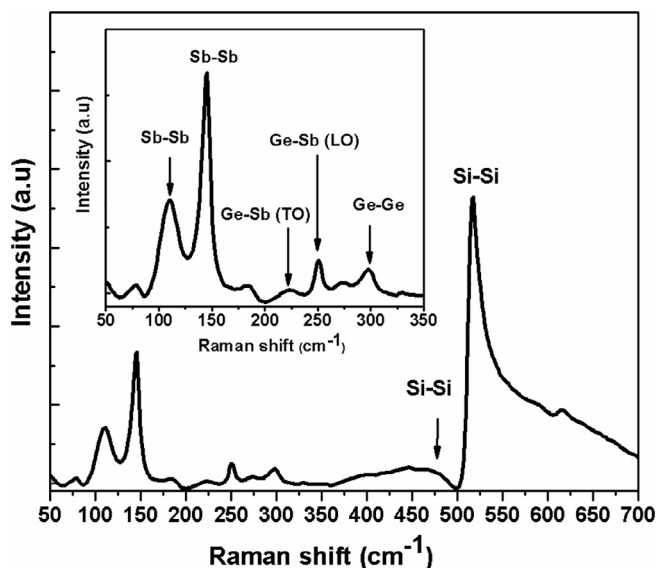


Fig. 3. Raman spectra of $\text{Ge}_{15}\text{Sb}_{85}$ Quantum dots deposited on Si substrate, and inset Fig. Raman spectrum between 50 and 350 cm^{-1} .

quantum dots (QDs) were fabricated by using a dc magnetron sputtering and inert gas condensation inside an ultra-high vacuum compatible system (UHV). The system consists of source and main chambers that are pumped down to a base pressure of 10^{-6} Pa. The QDs were produced from a composite target that was fixed on the sputtering head. Sputtering was operated by applying a dc voltage to the composite target in the presence of Argon (Ar) inert gas. (Ar) was used to produce the plasma required for sputtering, establish the inert-gas condensation,

and generate pressure gradient that enables QDs to travel from the source chamber (high pressure) to the deposition chamber (low pressure) [17].

To produce the QDs, a discharge power of 15 W was used during sputtering. The size of the quantum dots can be controlled by varying the Argon flow rate used to condensate the sputtered atoms and the distance between the target and the nozzle of the source (aggregation length) [7,18]. In this work, the Argon flow rate used is 60 sccm, and aggregation length $L = 50$ mm. The produced QDs were deposited on different substrates fixed on a sample holder located in the main chamber. The height and density of the deposited GeSb QDs were analyzed using AFM (Nanotec S.L, Madrid). In order to get the phonon vibration study of the GeSb quantum dots, an XploRA confocal Raman microscope (Horiba JobinYvon, France) was used with laser excitation of 532 nm.

Results and discussion

The AFM images and profiles of the samples surfaces reveal the density and height of the produces Quantum dots for different deposition time. Fig. 1(a) represents AFM topographic image of quantum dots on mica substrate for short time deposition, where distinct spherical QDs and their dispersion are observed. Height analysis of the QDs is shown in Fig. 1(b) and it was measured between 1.6 and 2.8 nm. Also, Quantum dots as three dimensional projections for low density displayed in Fig. 1(c). Fig. 2(a) represents AFM topographic image of quantum dots on mica substrate for long time deposition where one can observe distinct spherical QDs and their aggregates. Height analysis of these QDs shown in Fig. 2(b) and it was measured between 2.6 and 3.1 nm. It is noticeable that increasing the time of deposition leads to an increase in the height of QDs and becomes more aggregated. In addition, QDs as three dimensional projections of high density displayed in

Fig. 2(c).

In order to complement the topographic information provided by AFM images and understand the crystallinity of GeSb, Raman spectroscopy experiments were performed. Raman spectroscopy is considered one of the best methods for providing information about the crystallization by probing laser to modify the surface of materials. Fig. 3 shows Raman spectra of Ge-Sb quantum dots in low – frequency range. Raman spectroscopy measurements reveal that Ge-Sb phonon is positioned at 250 cm^{-1} (Lo mode) and 220 cm^{-1} (To mode). Also, a strong Sb-Sb peak is found at about 145 cm^{-1} and 110 cm^{-1} . Huang and coworkers showed that the crystallized eutectic Ge-Sb thin film strong Sb-Sb peaks are found at about 150 cm^{-1} and 110 cm^{-1} which did not appear in Raman spectra of the amorphous Ge-Sb thin films [19]. Furthermore, a significant peak appears at 290 cm^{-1} assigned to Ge-Ge modes [20]. In addition, there are features in Raman spectrum arises from Si substrate. These consist of abroad peak at 480 cm^{-1} due to stretching modes of Si-Si bonds and a sharp peak at 520 cm^{-1} due to the Si substrate.

Conclusion

Ge-Sb alloy QDs deposited on mica, Si, and quartz glass substrates have been successfully fabricated by magnetron sputtering with inert gas condensation. The Ge-Sb QDs have been characterized by Atomic force microscopy and Raman spectroscopy techniques. The size and density of Ge-Sb QDs can be varied by changing the deposition time. Raman spectroscopy measurements show that strong Sb-Sb crystallized peaks positioned at about 110 and 145 cm^{-1} . The growth of phase-change materials into nanostructures is very essential for nano-scale device application, and our magnetron sputtering with inert gas condensation has demonstrated the potential solution compare to chemical synthesis or top-down fabrication.

Acknowledgement

The authors are thankful for the financial support from Palestinian Technical University (PTUK).

References

- [1] Kolobov AV, Tominaga J, Fons P. Springer Handbook of Electronic and Photonic Materials. Cham: Springer International Publishing; 2017. 1 1.
- [2] Kellner J, Bihlmayer G, Liebmann M, Otto S, Pauly C, Boschker JE, et al. Commun Phys 2018;1:5.
- [3] Márquez E, Wagner T, González-Leal JM, Bernal-Oliva AM, Prieto-Alcón R, Jiménez-Garay R, et al. J Non-Cryst Solids 2000;274:62–8.
- [4] Raoux S, Cabral C, Krusin-Elbaum L, Jordan-Sweet JL, Virwani K, Hitzbleck M, et al. J Appl Phys 2009;105:064918.
- [5] Greer AL, Mathur N. Nature 2005;437:1246–7.
- [6] Yoon, D.H., Muralimanohar, N., Chang, J., Ranganathan, P., Jouppi, N.P., Erez, M., in: 2011 IEEE 17th International Symposium on High Performance Computer Architecture, 2011, pp. 466–477.
- [7] Mahmoud ST, Ayeshe AI, Qamhieh NN, Ahmad SJ. J Appl Phys 2012;112:034308.
- [8] Sun, X., Yu, B., NSTI-Nanotech 2007, ISBN1420061828 Vol.1 (2007).
- [9] Chen B, ten Brink GH, Palasantzas G, Kooi BJ. Sci Rep 2016;6.
- [10] Ramachandran S, Bishop SG. Appl. Phys. Lett. 1998;74:13–5.
- [11] Carlos R, Virgilio, Rivera, Eduardo Morales S, Jesús González H, Evgen P, Juan Mu –noz S, Gerardo Trapaga M. J. Surf. Eng. Mater. Adv. Technol. 2012. 2012.
- [12] Xu J, Almeida RM. J Sol-Gel Sci Technol 2000;19:243–8.
- [13] Bouška M, Pechev S, Simon Q, Boidin R, Nazabal V, Gutwirth J, et al. Sci Rep 2016;6:26552.
- [14] Gholipour B, Huang C-C, Ou J-Y, Hewak DW. Physica Status Solidi (b) 2013;250:994–8.
- [15] Chen B, de Wal D, ten Brink GH, Palasantzas G, Kooi BJ. Cryst Growth Des 2018;18:1041–6.
- [16] Pérez-Tijerina, E., Pinilla, M.G. Mejía-Rosales, S. Ortiz-Méndez, U., Torres, A., José-Yacamán, M. 353–362 2008 discussion 421–434.
- [17] Ayeshe AI, Qamhieh N, Ghamlouche H, Thaker S, El-Shaer M. J Appl Phys 2010;107:034317.
- [18] Ayeshe AI. Thin Solid Films 2017;636:207–13.
- [19] Huang CC, Gholipour B, Knight K, Ou JY, Hewak DW. Adv OptoElectron 2012;2012:1–7.
- [20] Rouchon D, Mermoux M, Bertin F, Hartmann JM. J Cryst Growth 2014;392:66–73.